Colloidal Dispersions of Gold Rods Characterized by Dynamic Light Scattering and Electrophoresis

ARTICLE *in* LANGMUIR · JANUARY 2000

Impact Factor: 4.46 · DOI: 10.1021/la990043x · Source: OAI

4 AUTHORS, INCLUDING:

Bianca van der Zande
Philips
23 PUBLICATIONS **1,152** CITATIONS
SEE PROFILE

Albert P Philipse
Utrecht University
189 PUBLICATIONS **6,443** CITATIONS
SEE PROFILE

Colloidal Dispersions of Gold Rods Characterized by Dynamic Light Scattering and Electrophoresis

Bianca M. I. van der Zande,[†,‡] Jan K. G. Dhont,[†] Marcel R. Böhmer,*[,‡] and Albert P. Philipse[†]

Van't Hoff Laboratory for Physical and Colloid Chemistry, Debye Institute, Utrecht University, Padualaan 8, 3584 CH Utrecht, The Netherlands, and Philips Research Laboratories, Prof. Holstlaan 4, 5656 AA Eindhoven, The Netherlands

Received January 14, 1999. In Final Form: August 23, 1999

The colloidal stability of nearly monodisperse aqueous dispersions of rod-shaped gold particles is studied by dynamic light scattering and electrophoresis. The average length of the gold particles is adjusted between 39 and 730 nm, and the diameter is about 17 nm. The translational diffusion coefficients are consistent with calculations for single nonaggregated rods with a 10−15 nm thick poly(vinyl pyrrolidone) (PVP) adsorption layer. This supports the colloidal stability observed. Electrophoresis measurements show that the PVP-stabilized gold rods are negatively charged with a ζ potential of about −47 mV, which according to interaction calculations is sufficient for double-layer stabilization. Gold-sphere dispersions are investigated for comparison. It turns out that PVP-stabilized gold spheres have a ζ potential similar to that of the colloidal rods.

1. Introduction

In part 1[1] of this series we described the synthesis of colloidal gold rods using a nanoporous alumina membrane. Dispersions of the electrochemically grown gold rods have been obtained by successively dissolving the membrane and release of the rods from the substrate. At first sight the particles seem fairly stable: no aggregation or gelation is visually observed. In this paper we investigate the colloidal stability more quantitatively by dynamic light scattering (DLS) and electrophoresis. The aim is to verify whether our synthesis method indeed yields nonaggregated rods and to underpin this stability by interaction energy calculations.

For colloidal rods DLS yields both the translational and rotational diffusion coefficients, which both strongly depend on the particle size and shape.[2−6] Particle dimensions derived from DLS data will be different from the number-averaged particle dimensions determined by, e.g., transmission electron microscopy (TEM) when clustering or polydispersity exists. Therefore, DLS is a useful tool to monitor the presence of aggregates in the dispersion. In addition, DLS is sensitive to the hydrodynamic particle dimensions which are significantly increased by, e.g., adsorption of a polymer. In this study the diffusion coefficients are measured for a series of aspect ratios. Comparison to predictions using the equations of Garcia de la Torre[4] allows an estimation of the thickness of the PVP adsorption layer.

Colloidal stability is ensured by a high repulsive barrier in the interaction potential between particles. This repulsive barrier can be induced by steric or double-layer repulsion. The double-layer repulsion energy is according to the DLVO theory[7] proportional to the electrical surface potential squared. The surface potential can be estimated from the potential at the slip plane,[8,9] called the ζ potential. The ζ potential is, subsequently, deduced from the electrophoretic mobility, which is the measured quantity in an electrophoresis experiment. The absolute value for the ζ potential depends on the theoretical description of the electrophoretic mobility (whether, e.g., the relaxation force,[10,11] end effects,[12] or surface conduction[13] is taken into account). Although the ζ potential does not coincide with the surface potential, it has a predictive value with respect to colloidal stability, because a high ζ potential will always favor the double-layer repulsion. Electrophoresis, thus, gives insight into the repulsive interaction due to the double-layer repulsion.

For comparison to colloidal gold rods, we have also investigated dispersions of the more familiar gold spheres[14−16] with electrophoresis. For example, it is interesting to verify whether the gold spheres dispersed with the same stabilizer have ζ potentials identical with that of the colloidal gold rods. Additional evidence with respect to the colloidal stability of the rod dispersions is

* Corresponding author.
† Utrecht University.
‡ Philips Research Laboratory.

(1) van der Zande, B. M. I.; Böhmer, M R.; Fokkink, L. G. J.; Schönenberger, C. *J. Phys. Chem. B* **1997**, *101*, 852. van der Zande, B. M. I.; Böhmer, M R.; Fokkink, L. G. J.; Schönenberger, C. *Langmuir* **2000**, *16*, 451.
(2) van Bruggen, M. P. B.; Lekkerkerker, H. N. W.; Dhont, J. K. G. *Phys. Rev. E* **1997**, *56*, 4394.
(3) Kluijtmans, S. G. J. M.; Koenderink, G.; Philipse, A. P. **1998**, in preparation.
(4) Garcia de la Torre, J.; Bloomfield, V. A. *Q. Rev. Biophys.* **1981**, *14*, 81.
(5) Dhont, J. K. G. *An introduction to dynamics of colloids*; Elsevier: Amsterdam, The Netherlands, 1996.
(6) Zero, K. M.; Pecora, R. *Macromolecules* **1982**, *15*, 87.
(7) Israelachvili, J. N. *Intermolecular and surface forces, with applications to colloidal and biological systems*; Academic Press: London, 1985.
(8) Lyklema, J. *Fundamentals of interface and colloid science, Vol II solid−liquid interfaces*; Academic Press: London, 1995.
(9) Hunter, R. J. *Zeta potential in colloid science*; Acadamic Press: London, 1981.
(10) O'Brien, R. W.; White, L. R. *J. Chem. Soc., Faraday Trans. 2* **1978**, *74*, 1607.
(11) Stigter, D. *J. Phys. Chem.* **1978**, *82*, 1417; **1978**, *82*, 1424.
(12) Sherwood, J. D. *J. Chem. Soc., Faraday Trans. 2* **1982**, *78*, 1091.
(13) Minor, M. Electrophoresis of colloids. Thesis, Landbouwuniversiteit Wageningen, The Netherlands, 1998.
(14) Chow, M. K.; Zukoski, C. F. *J. Colloid Interface Sci.* **1994**, *165*, 97.
(15) Enüstün, B. V.; Turkevich, J. *J. Am. Chem. Soc.* **1963**, *85*, 3317.
(16) Biggs, S.; Mulvaney, P.; Zukoski, C. F.; Grieser, F. *J. Am. Chem. Soc.* **1994**, *116*, 9150.

10.1021/la990043x CCC: $19.00
Published on Web 11/16/1999

Table 1. Characteristics of the Template-Synthesized Gold Rods Dispersed in an Aqueous Medium[a]

system	length (L; nm)	σ_L (nm)	diameter (d; nm)	σ_d (nm)	L/d
SPHERE18	18	5			
SPHERE15	15	3			
ROD2.6a	47	17	18	3	2.6
ROD2.6b	39	10	15	3	2.6
ROD8.9	146	37	17	3	8.9
ROD12.6	189	24	15	3	12.6
ROD14	283	22	20	3	14
ROD17.2	259	60	15	2	17.2
ROD17.4	279	68	16	3	17.4
ROD39	660	68	17	3	39
ROD49	729	20	15	3	49

[a] The particle dimensions are determined by analysis of the TEM micrographs. σ_x:the standard deviation of x.

obtained by confocal scanning laser microscopy (CSLM)[17] and visible near-infrared (vis/NIR) spectroscopy.[1]

2. Experimental Section

2.1. Colloidal Dispersions of Rod-Shaped Gold Particles. Colloidal dispersions of rod-shaped gold particles with aspect ratios in the range $2.5 < L/d < 49$ were synthesized by electrodeposition of gold in nanopores of anodized alumina.[1] The obtained particles were dispersed in an aqueous medium by dissolving the membrane and release of the substrate. Poly(vinylpyrrolidone) (PVP; M_w = 40 000, Fluka) served as the stabilizer. For detailed information concerning the preparation of rod-shaped gold particles, we refer to part 1. Dispersions of spherical particles were prepared following the method of Frens.[18] PVP was added to the citrate-stabilized dispersion to obtain PVP-stabilized gold spheres which are used as a reference. The final concentration of PVP in the spherical gold sols was 0.4 mg·mL^{-1}.

Table 1 summarizes the number-averaged particle dimensions determined by analysis of the transmission electron micrographs. The synthesized rod dispersions are coded as, for instance, ROD2.6, where the number refers to the aspect ratio. The dimensions of the gold spheres are given in Table 1 as well. The sphere dispersions are labeled as SPHERE15 and SPHERE18. The number-averaged sphere diameter was determined by TEM in combination with image analysis.

The DLS and electrophoresis measurements were performed on dilute samples with a gold concentration of 6−40 mg·L^{-1}. The volume percentages were so low that particle interactions can be neglected.[19−21] This is important because the presented DLS and electrophoresis equations are only valid for infinite dilutions.

2.2. DLS. DLS measurements were performed with a Spectra Physics series 2020 krypton laser operating at a wavelength of 647.1 nm. This wavelength was chosen to minimize the absorption of light by gold dispersions and, consequently, to avoid convection due to heating of the particles. Normalized intensity autocorrelation functions (IACF) were measured with a Malvern Multi 8 7032 CE 128-point correlator. The scattering angles ranged from 30° to 120°, and the sample was thermostated at $T = 298$ K. Measurements were performed in the VV mode (vertical−vertical mode) and in the VH mode (vertical−horizontal mode).[3−5] In the VV mode both the incident and detected scattered light are polarized perpendicular to the plane spanned by the incident and detected wavevectors. In the VH mode the scattered intensity is polarized within the plane spanned by the incident and detected wavevectors. Consequently, the fluctuations of the depolarized component of the scattered intensity are probed, which are sensitive to both rotational and translational motion.

The IACFs were fitted to single exponents including a second cumulant ($c(k)$) to account for polydispersity:[5]

$$y = \alpha + \beta \exp(-b(k)\, t + c(k)\, t^2) \qquad (1)$$

with t the time, α and β fit parameters, and k the wavevector of light defined as

$$k = \frac{4\pi n}{\lambda} \sin\left(\frac{\theta}{2}\right) \qquad (2)$$

where θ is the scattering angle, n the refractive index of the medium, and λ the wavelength of light in a vacuum.

In the VV mode the decay exponent ($b(k)$) corresponds to

$$b(k) = 2D_t k^2 \qquad (3)$$

and in the VH mode to

$$b(k) = 2D_t k^2 + 12D_r \qquad (4)$$

provided that $kL < 5$ and that the particles are optically isotropic.[5,22] Here D_t represents the translational diffusion coefficient, whereas D_r is the rotational diffusion coefficient.

2.3. Electrophoresis. The electrophoretic mobility was measured on the Zetasizer 4 (Malvern) thermostated at 298 K. An alternating electric field is used at such a frequency that the electroosmosis is suppressed.[23] Electrophoresis measurements were also performed with a Coulter DELSA 440SX (Doppler Electrophoretic Light Scattering Analyzer of Langley Ford Instruments Division of Coulter Electronics of New England, Inc.) thermostated at 298 K.

The measured electrophoretic mobility is converted in a ζ potential using the expression of Hückel:[22,24]

$$\mu = \frac{2}{3}\epsilon\zeta/\eta \qquad \text{for } \kappa a \ll 1 \qquad (5)$$

Here, the viscosity is represented by η and ϵ is the static dielectric constant of the medium. The Debye length (κ^{-1}) characterizes the double-layer thickness around a charged particle in an electrolyte solution

$$\kappa^{-1} = \sqrt{\frac{\epsilon kT}{e^2 I_s}} \qquad (6)$$

with kT the thermal energy and I_s the ionic strength

(17) van der Zande, B. M. I.; Pagès, L.; Hikmet, R. A. M.; van Blaaderen, A. *J. Phys. Chem. B* **1999**, *103*, 5761.
(18) Frens, G. *Nature* (*London*), *Phys. Sci.* **1973**, *241*, 20.
(19) Doi, M.; Edwards, S. F. *J. Chem. Soc., Faraday Trans. 2* **1978**, *74*, 560.
(20) Doi, M.; Edwards, S. F. *J. Chem. Soc., Faraday Trans. 2* **1978**, *74*, 918.
(21) Wierenga, A. M.; Philipse, A. P. *Langmuir* **1997**, *13*, 4574.
(22) van der Zande, B. M. I. Colloidal dispersions of gold rods, synthesis, characterization and optical properties. Thesis, Utrecht University, Utrecht, The Netherlands, 1998.
(23) Minor, M.; van der Linde, A. J.; van Leeuwen, H. P.; Lyklema, J. *J. Colloid Interface Sci.* **1997**, *189*, 370.
(24) Hückel, E. *Phys. Z.* **1924**, *25*, 204.

$$I_s = \frac{1}{2}\sum z_i^2 n_i \quad (7)$$

in which z_i is the valence of ions of type i and n_i the number density of ions of type i.

3. Results and Discussion

3.1. DLS. *Diffusion Coefficients*. The measured IACFs for the dispersions of rods with $L/d \geq 8.9$ can be fitted with cumulant fits (eq 1). A typical IACF together with its fit is given in Figure 1. In Figure 2 the fit parameter $b(k)$ is plotted as a function of k^2 for the dispersions ROD8.9 and ROD39. Subsequently, the translational diffusion coefficients of the dispersions are determined from the slope of the linear fit through the data points ($b(k)$) in the VV mode as well as in the VH mode. The rotational diffusion coefficients are determined from the intercept of the linear fit obtained in the VH mode. The results are summarized in Table 2. As expected the diffusion coefficient depends on the aspect ratio: an increase in the particle length results in a decrease in the diffusion coefficient.

The decay exponent ($b(k)$) of the dispersions ROD39 and ROD49 shows a significant deviation from the linear dependence at higher values of k^2. Figure 2 illustrates this deviating behavior for ROD39. This deviation is attributed to the rotational coupling.[1,5] Therefore, D_t and D_r are determined from the slope of the linear fit through the data points with $k^2 < 2 \times 10^{14}$ m^2. At this wavevector kL is about 9. The DLS results for the dispersion ROD14 show that $b(k)$ depends linearly on k^2. The maximum value of kL in this experiment is about 6. Apparently, the theoretical value $kL > 5$ at which coupling plays a role is not very critical.

The IACFs for the dispersions SPHERE and ROD2.6 cannot be fitted with a single exponent because of polydispersity. According to TEM data, the system ROD2.6 contains rod-shaped particles, ellipsoids, and spherical particles. The presence of several particle shapes in one dispersion may lead to a scattering behavior which cannot be described by only one single exponent.

Comparison of the Diffusion Coefficients with the Theory. According to Garcia de la Torre et al.,[4] the translational diffusion coefficient D_t for Brownian rods with a finite aspect ratio (L/d) can be expressed as

$$D_t = \frac{kT}{3\pi\eta L}\left[\ln\left(\frac{L}{d}\right) + 0.312 + 0.565\frac{d}{L} + 0.100\left(\frac{d}{L}\right)^2\right] \quad (8)$$

and the rotational diffusion coefficient D_r as

$$D_r = \frac{3kT}{\pi\eta L^3}\left[\ln\left(\frac{L}{d}\right) - 0.662 + 0.917\frac{d}{L} - 0.050\left(\frac{d}{L}\right)^2\right] \quad (9)$$

with L the average particle length and d the average diameter.

According to eqs 8 and 9, both diffusion coefficients depend mainly on the particle length. Therefore, the translational diffusion coefficient (D_t) is plotted versus $1/L$, and the rotational diffusion coefficient (D_r) is plotted versus $1/L^3$ in Figure 3. This figure (as well as Table 2) includes the calculations for D_t and D_r using the equations of Garcia de la Torre[4] for smooth cylinders and the number-averaged TEM dimensions. The $1/L$ dependence on the experimental D_t agrees qualitatively with that calculated.

The absolute values of the diffusion coefficients, however, deviate from the calculations. The experimental D_t at infinite dilution is approximately twice as low as those calculated using eqs 8 and 9. The deviation between

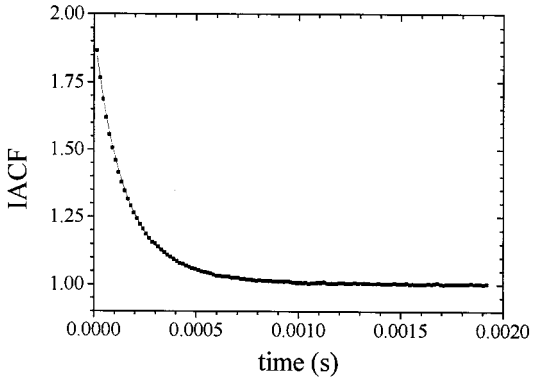

Figure 1. Typical VV-polarized intensity autocorrelation function (IACF) plotted against the time, together with its fit for dispersion ROD8.9 at $k^2 = 7.19 \times 10^{14}$ m^2.

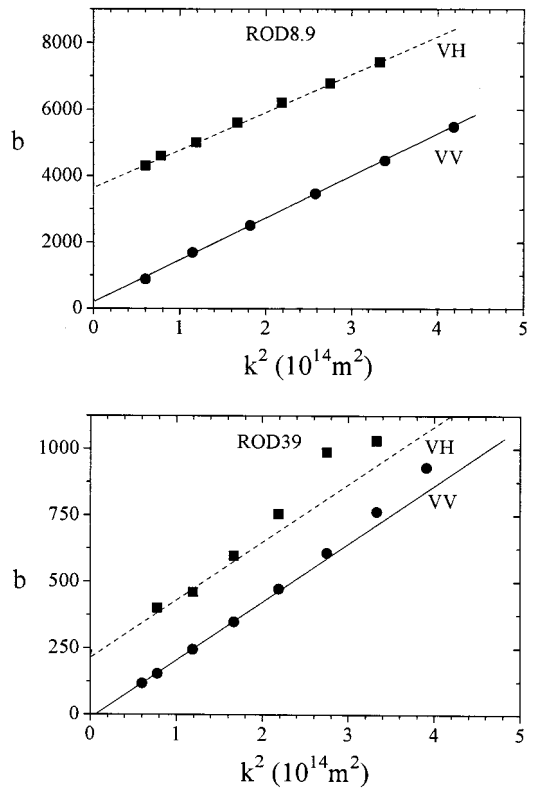

Figure 2. Fitted decay exponent $b(k)$ of the DLS intensity autocorrelation function as a function of the wavevector squared, k^2, for ROD8.9 and ROD39. The solid line indicates the linear fit through the data points obtained in the VV mode. The dotted line represents the linear fit through the data points obtained in the VH mode.

calculation and experiment in D_r is a factor of 3 for $L/d = 39$ up to a factor of 8 for $L/d = 8.9$. This discrepancy can be explained by the PVP adsorption layer which leads to an increase in the hydrodynamic volume. Figure 4 shows the effect of a PVP adsorption layer on the diffusion coefficients. In this figure the diffusion coefficients are calculated with eqs 8 and 9 including a PVP adsorption layer with a thickness δ in the average TEM dimensions (i.e., $L + 2\delta$, $d + 2\delta$). The PVP adsorption layer reduces the diffusion coefficients significantly. When a PVP adsorption layer with a thickness $\delta = 10-15$ nm, which is a reasonable estimate,[25,26] is included in the calculations,

(25) Fleer, G. J.; Cohen Stuart, M. A.; Scheutjens, J. H. H. M.; Cosgrove, T.; Vincent, B. *Polymers at Interfaces*; Chapman and Hall: London, 1993.

(26) Cohen Stuart, M. A.; Mulder, J. W. *Colloids Surf.* **1985**, *15*, 49.

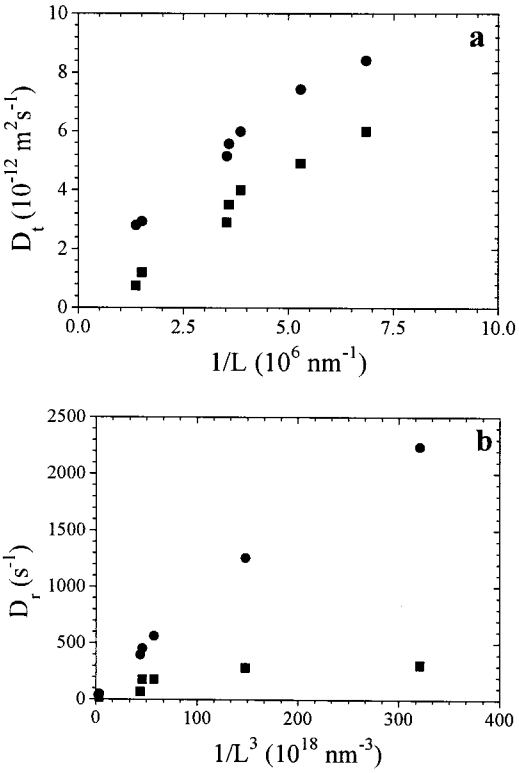

Figure 3. (a) Measured translational diffusion coefficient (D_t) plotted against the inversed length ($1/L$). (b) Rotational diffusion coefficient (D_r) plotted against the inversed cubic length ($1/L^3$). The figures include the diffusion coefficients calculated with eqs 8 and 9 using the dimensions as determined by TEM analysis. The experimental and calculated diffusion coefficients are indicated with the symbols ■, and ●, respectively.

Table 2. Translational and Rotational Diffusion Coefficients Measured (exp) as Well as the Diffusion Coefficients Calculated (cal) with Eqs 8 and 9 Using the Dimensions As Determined by Analysis of the TEM Micrographs

	D_t (10^{-12} m^2 s^{-1})		D_r (s^{-1})	
system	exp	cal	exp	cal
ROD8.9	6.0	8.4	306	2238
ROD12.6	4.9	7.4	281	1258
ROD14	2.9	5.2	66	396
ROD17.2	4.0	6.0	177	563
ROD17.4	3.5	5.6	175	452
ROD39	1.2	2.93	13.7	46
ROD49	0.74	2.8		30

a much better agreement is found between the calculated and experimental diffusion coefficients.

3.2. Electrophoresis. *Electrophoretic Mobility*. Table 3 summarizes the electrophoretic mobilities (μ) and the conductivity of the medium (K^L). The mobilities measured on the Zetasizer are indicated with an asterisk and represent the averaged value over 15 measurements, while the mobilities measured on the Coulter DELSA (indicated with a pound sign) are obtained with the procedure described by Pelton et al.[27] The average mobility for the investigated gold rods is $-2.4 \times 10^{-8} \pm 0.41$ m^2·V^{-1}·s^{-1}. No significant discrepancy is found between the electrophoretic mobilities for the rod-shaped particles measured on the Zetasizer and the Coulter DELSA. The negative charge of the gold rods originates from specifically adsorbed anions such as CN^-, PO_4^{3-}, and SO_4^{2-} used in the preparation procedure; their presence has been confirmed by static SIMS measurements on rods still attached to the plating base.[1,22]

The mobility signal obtained for gold spheres is noisy, and the distribution of mobilities around the average mobility is broad in contrast to the mobility signal of gold rod dispersions. These effects are due to the small sphere size and, consequently, diffusional broadening and weak light scattering occurred. Nevertheless, the average mobility was reproducible. In addition, the electrophoretic

(27) Pelton, R.; Miller, P.; McPhee, W.; Rajaram, S. *Colloid Surf. A* **1993**, *80*, 181.

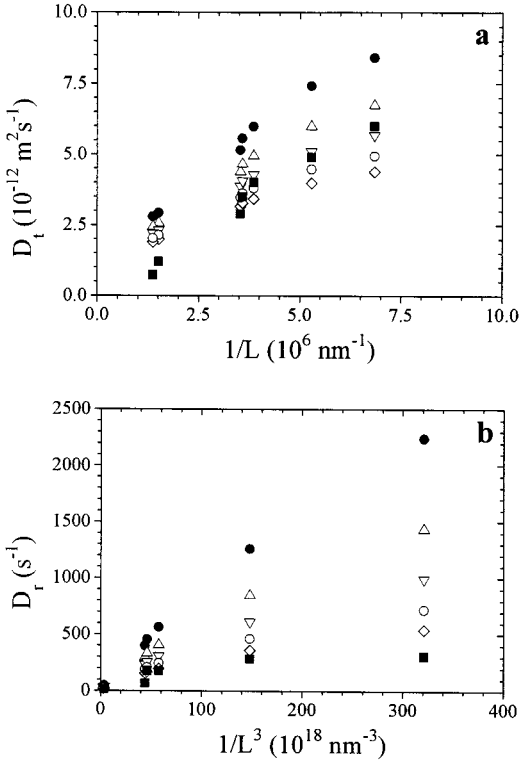

Figure 4. Translational (a) and rotational (b) diffusion coefficients calculated with eqs 8 and 9 using the dimensions as determined by TEM analysis incorporating a polymer adsorption layer. The calculation results of a polymer adsorption layer with a thickness of $\delta = 0$ (●), 5 (△), 10 (▽), 15 (○), and 20 nm (◇) are given. The experimental results (■) are also shown.

Table 3. Electrophoretic Data[a]

system	K^L (10^{-3} S/cm)	κ^{-1} (nm)	κa	κL	μ (10^{-8} m^2/V s)	ζ (mV)
SPHERE18#	0.204	7	1.27		−4.3#	−81
					−4.2#	−78
SPHERE15#	0.288	6	1.29		−3.8#	−79
SPHERE18PVP#	0.7	4	2.34		−1.2#	−25
SPHERE15 PVP#	0.288	6	1.29		−1.7#	−31
ROD2.6a#	0.0544	14	0.65	3.4	−2.9#	−55
ROD2.6b*	0.0423	15	0.43	2.6	−2.5*	−47
	0.0591	13	0.49	3	−2.2*	−42
ROD8.9#	0.0644	12	0.67	12	−2.0#	−40
	0.0588	14	0.62	11	−1.8#	−37
ROD12.6*	0.0445	15	0.50	13	−2.6*	−49
	0.0340	17	0.25	11	−2.7*	−52
ROD17.2*	0.0410	16	0.48	17	−2.3*	−47
ROD17.4*	0.0230	20	0.17	13	−2.9*	−55
	0.0343	17	0.44	16	−3.0*	−58
ROD39#	0.01341	28	0.31	24	−2.2#	−42
ROD49*	0.0553	14	0.45	53	−1.9*	−36

[a] The electrophoretic mobility (μ) is converted to a ζ potential (ζ) using eq 5.[22,24] The Debye length κ^{-1} is estimated from the conductivity of the medium (K^L).[31] *: measured on the Zetasizer. #: measured on the Coulter DELSA. *a*: particle radius. *L*: particle length.

mobility for citrate-stabilized gold spheres equals the mobility measured by Chow et al.[14] for a similar system.

ζ Potential. In the conversion of mobilities to ζ potentials, we assume that the gold colloids are uniformly charged and that the electric field is too low to align the rod-shaped particles.[28] Consequently, the measured mobility can be treated as an orientationally averaged mobility.[29] Table 3 summarizes the ζ potentials calculated with eq 5. The thus-obtained ζ potential of PVP-stabilized gold rods is independent of the aspect ratio and equals -47 ± 7 mV. The independence of the ζ potential of the aspect ratio complies with Sherwood's analysis,[12] which is valid for arbitrary κL and $\kappa a \ll 1$. The numerical results[12] approach Henry's results for infinitely long rods when $\kappa L > 5$. This condition is fulfilled for all of the dispersions except for the systems ROD2.6. Possibly, end effects play a role in the measured mobility, but no deviating electrophoretic behavior is found.

The effect of a PVP adsorption layer on the ζ potential is clearly demonstrated by the mobility results obtained for the PVP-stabilized gold spheres. The mobility is much lower than for that the citrate-stabilized spheres which is caused by outward shift of the slip plane due to the presence of adsorbed polymer. Consequently, the ζ potential of PVP-stabilized spheres is lower than that of citrate-stabilized spheres, although it is likely that the specific adsorption of ions on the gold surface does not differ significantly. The ζ potential of PVP-stabilized spheres is slightly less than that of PVP-stabilized rods. This indicates the synthesized gold rods to be colloidally stable considering that the PVP-stabilized spheres exhibit a long-term colloidal stability. Independent confirmation of PVP adsorption on gold was obtained using optical reflectometry in stagnation point flow on a 15 nm thick gold film on a silicon wafer. An adsorbed amount of about 0.6 mg/m^2 was found, and this amount did not change if a preadsorption step with citrate was performed.[22]

3.3. Colloidal Stability. Because the measured IACFs for the rod dispersions with an aspect ratio $L/d \geq 8.9$ can be fitted with a single exponent (Figure 1), the majority of the rods are freely diffusing particles which do not form aggregates.[5] Furthermore, polydispersity or parallel aggregates are virtually absent in dilute dispersions of gold rods, because for all dispersions the diffusion coefficient is virtually independent of the wavevector squared, as is shown in Figure 5. Any significant polydispersity or (parallel) aggregation leads to a decrease in diffusion coefficient especially at small k values.[2,5] The DLS data (see Figures 1−3) distinctly show that the dynamical behavior of single particles is measured. Therefore, the colloidal dispersions of gold rods investigated can be considered as colloidally stable. We also note here that for one dispersion (ROD17.2) the DLS experiments were repeated after 6 months. The same results were found.

In addition, the electrophoresis experiments show that the gold rods are negatively charged. The repulsive interaction required for colloidal stability may originate from double-layer interactions combined with sterical interactions caused by the PVP adsorption layer. To verify whether $\zeta = -47$ mV will lead to colloidal stability when only the double-layer repulsion is taken into account, we have calculated the interaction energy between gold rods using the expressions of Sparnaay[30] for the double-layer repulsion and the van der Waals attraction as given by Israelachvili[7] for two parallel cylinders. The energy barrier layer and the secondary minimum are such that colloidal stability is predicted as shown in Figure 6. The calculated double-layer repulsion underestimates the actual repulsion between the gold rods because the location of the slip plane is not taken into account in the interaction energy calculation. The dotted vertical line in Figure 6 indicates

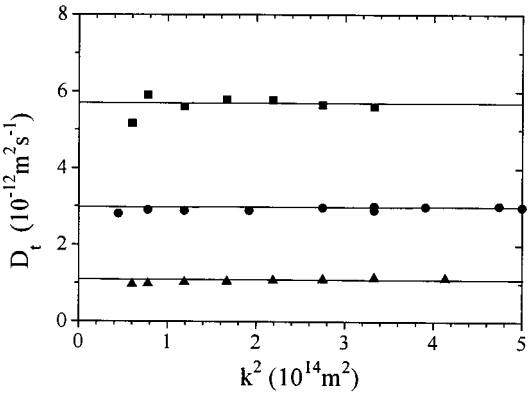

Figure 5. Translational diffusion coefficient (D_t) plotted against the wavevector squared, k^2. The symbols ▲, ●, and ■ represent the diffusion coefficients per wavevector squared of the dispersions ROD39, ROD14, and ROD8.9, respectively. Horizontal lines are drawn through the data points to guide the eye.

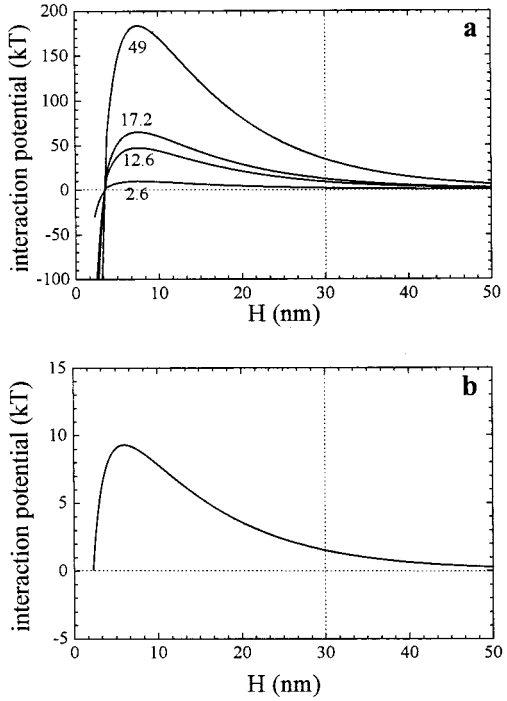

Figure 6. Interaction potential for two gold rods in water as a function of the surface-to-surface distance (H) calculated for both parallel (a) and crossed (b) orientations. The numbers on the curves represent the aspect ratio. The diameter is 15 nm, which results in one single curve for the crossed orientation. The monovalent salt concentration is taken to be 0.5 mM, which is approximately the experimental condition. The Hamaker constant[16] is assumed to be 60 kT at $T = 298$ K, and for the surface potential, the experimental value for the ζ potential (−47 mV) is used. The dotted vertical line represents the minimal surface-to-surface distance in the presence of a 15 nm thick PVP adsorption layer.

(28) van der Zande, B. M. I.; Koper, G. J. M.; Lekkerkerker, H. N. W. *J. Phys. Chem. B* **1999**, *103*, 5754.

(29) de Keizer, A.; van der Drift, W. P. J. T.; Overbeek, J. Th. G. *Biophys. Chem.* **1975**, *3*, 107.

(30) Sparnaay, M. J. *Recl. Trav. Chim. Pays-Bas* **1959**, *78*, 680.

(31) Kramer, H.; Graf, C.; Hagenbüchle, M.; Johner, C.; Martin, C.; Schwind, P.; Weber, R. *J. Phys. II Fr.* **1994**, *4*, 1061.

the minimum surface-to-surface distance in the presence of an adsorption layer with a thickness of 15 nm. The use of the measured ζ potential as surface potential indicates that double-layer interactions give a significant contribution to the repulsion.

4. Conclusions

We conclude that gold rods prepared according to the method described in part 1[1] form stable nonaggregated dispersions. Comparison of the measured translational and rotational diffusion coefficients with the calculations for free rods demonstrates the presence of nonaggregated rods and a PVP adsorption layer with a thickness of about 10−15 nm. In addition, electrophoresis reveals that the gold rods are negatively charged, with a ζ potential of −47 mV which is similar to the ζ potential of colloidally stable gold spheres with a PVP adsorption layer. Calculation of the double-layer interaction energy confirms that a ζ potential of −47 mV is sufficient to stabilize the gold particles under the conditions studied. Both steric and double-layer repulsion contribute to the colloidal stability.

Acknowledgment. Dr. M. J. M. J. Severens (Centre For manufacturing Technology, Philips, Eindhoven, The Netherlands) is acknowledged for his assistance with the electrophoresis measurements on the Zetasizer. Dr. J. Sherwood (Schlumberger Cambridge Research) and Dr. Y. Solomentsev (Carnegie Mellon University, Pittsburgh) are thanked for their comments on the interpretation of the electrophoretic mobilities. Dr. M. P. B. van Bruggen (Van't Hoff laboratory for Physical and Colloid Chemistry, Utrecht University, Utrecht, The Netherlands) is thanked for providing the computer program to calculate the interaction potential. Prof. Dr. H. N. W. Lekkerkerker (Van't Hoff laboratory for Physical and Colloid Chemistry) and Dr. Ir. L. G. J. Fokkink (Philips Research Laboratories) are acknowledged for stimulating discussions. This work is part of the research program of the Foundation for Fundamental Research on Matter (FOM) with financial support from The Netherlands Organization for Scientific Research (NWO).

LA990043X